

Article

Assessment of Antioxidant Activity of Pure Graphene Oxide (GO) and ZnO-Decorated Reduced Graphene Oxide (rGO) Using DPPH Radical and H₂O₂ Scavenging Assays

Nacera Baali ^{1,*}, Assia Khecha ², Aicha Bensouici ^{2,*}, Giorgio Speranza ³ and Noudjoud Hamdouni ⁴

¹ Department of Animal Biology, Mentouri Brothers University, Constantine 25000, Algeria

² Laboratory of Mathematical and Subatomic Physics, Department of Physics, Mentouri Brothers University, Constantine 25000, Algeria; assiakhecha@gmail.com

³ FMPS-CMM, Fondazione Bruno Kessler, 38123 Trento, Italy; speranza@fbk.eu

⁴ Laboratory of Crystallography, Department of Physics, Mentouri Brothers University, Constantine 25000, Algeria; n_hamdouni@yahoo.fr

* Correspondence: nacirabek@hotmail.com (N.B.); bensouicia@yahoo.fr (A.B.);
Tel.: +213-31811173 (N.B. & A.B.)

Received: 11 October 2019; Accepted: 15 November 2019; Published: 18 November 2019



Abstract: In this work, zinc oxide-decorated graphene oxide (ZnO-rGO) was successfully synthesized with a fast reflux chemical procedure at 100 °C. An equal mass ratio of graphene oxide (GO) and zinc acetate was used as starting materials dissolved, respectively, in ultrapure distilled water and dimethylformamide (DMF). Particularly, pure GO was synthesized using Hummers modified protocol by varying the mass ratio of (graphite:potassium permanganate) as follows: 1:2, 1:3, and 1:4, which allow us to obtain six types of pure and decorated samples, named, respectively, GO1:2, GO1:3, GO1:4, ZnO-rGO1:2, ZnO-rGO1:3, and ZnO-rGO1:4 using reflux at 100 °C. X-ray diffraction, FTIR, and Raman spectroscopy spectra confirm the formation of wurzite ZnO in all ZnO-decorated samples with better reduction of GO in ZnO-rGO1:4, confirming that a higher degree of graphene oxidation allows better reduction during the decoration process with ZnO metal oxide. Antioxidant activity of pure and zinc oxide-decorated graphene oxide samples were compared using two different in vitro assays (DPPH radical and H₂O₂ scavenging activities). Considerable in vitro antioxidant activities in a concentration-dependent manner were recorded. Interestingly, pristine GO showed more elevated scavenging efficiency in DPPH tests while ZnO-decorated GO was relatively more efficient in H₂O₂ antioxidant assays.

Keywords: GO; ZnO-rGO; antioxidant activity; DPPH radical; H₂O₂ assay

1. Introduction

During recent decades, the emergence of carbon nanomaterials in nanoscience opens an important research field for all Carbon allotropes [1]. Graphene, an atomically thin two-dimensional carbonaceous material, has attracted tremendous attention in the scientific community due to its exceptional electronic, electrical, and mechanical properties [2,3]. Graphene-based materials have gained heightened attention as novel materials for water treatment, environmental remediation, and medical applications (e.g., biosensors, bioimaging, and drug delivery) [4,5]. Indeed, with the recent explosion of methods for large-scale synthesis of graphene, the number of publications related to graphene and other graphene-based materials has increased exponentially. Usually, graphene production could be done

using the exfoliation-reduction of graphene oxide (GO) in an acid medium. Brodie first demonstrated the synthesis of GO in 1859 by adding a portion of potassium chlorate to a slurry of graphite in fuming nitric acid. In 1898, Staudenmaier improved on this protocol by using a mixture of concentrated sulfuric acid and fuming nitric acid followed by the gradual addition of chlorate to the reaction mixture. In 1958, Hummers modulated the GO synthesis protocol and used potassium permanganate (KMnO_4) and NaNO_3 in concentrated sulfuric acid (H_2SO_4) [6]. In recent years, the Tour process has been proposed as an alternative to Hummers' method, aiming to minimize toxic gas production and control the synthesis conditions [7]. As its unparalleled properties, including high surface area, excellent conductivity, ease of functionalization, and production, graphene provides an ideal platform to make useful nanomaterials, and motivates researchers to synthesize metallic nanoparticle-graphene nanocomposites for fabricating sensors and biosensors and enhancing performance [8,9]. Moreover, GO could be used as 2D matrices decorated by chemical elements or metal oxides, for example, to obtain metal oxide-reduced graphene oxide [10]. Loading of gold nanoparticles (AuNPs) or silver nanoparticles (AgNPs) in the graphene sheets enhanced the photocatalytic activity of the Au-graphene, and Ag-graphene nanocomposite. The synergistic effects of the surface plasmonic resonance of AuNPs or the hydrophilic nature of the Ag-graphene nanocomposite and the specific electronics effect of graphene holds great promise for adsorption and photocatalysis application [2,11]. Additionally, zinc oxide (ZnO) nanoparticle-decorated graphene nanosheets are considered as an advanced material for their electrochemical performance and photocatalytic degradation of organic dyes [12,13]. Under such conditions, ZnO can act as a photocatalyst while graphene acts as an electron-acceptor/transport material to facilitate the migration of photogenerated electrons and hinders electron-hole recombination [12]. Furthermore, decorating the graphene surface with ZnO can be greatly improve their antibacterial and antioxidant properties [14].

In this work, a modified Hummers' method was used to optimize GO synthesis using H_2SO_4 and varying graphite: KMnO_4 proportion. Produced GO has been decorated with ZnO to obtain zinc oxide-decorated graphene oxide (ZnO-rGO). This work also verified the possible effect of the oxidation degree on the quality of GO decoration with Zn nanoparticles to obtain a good decoration of the GO sheet surfaces. Structural properties of pure GO and ZnO-rGO nanocomposites were studied using XRD, FTIR, and Raman spectroscopy. These techniques give us a semi-quantitative evaluation of reduction and decoration of GO and ZnO-rGO, respectively. The antioxidant activity of GO and ZnO-rGO nanocomposites was assessed using DPPH radical and H_2O_2 scavenging assays.

2. Materials and Methods

All chemicals, including graphite powder (with diameter < 20 μm , synthetic), potassium permanganate, zinc acetate dihydrate, L-ascorbic acid (99%), DPPH (2, 2-diphenyl-1-picrylhydrazyl), sulfuric acid (95–97%), hydrogen peroxide, and methanol were purchased from Sigma Aldrich (Sigma-Aldrich, St. Louis, MO, USA). All the chemicals used were of analytical grade and used without purification.

2.1. GO and ZnO-rGO Nanocomposites Synthesis and Characterization

GO synthesis was carried out using modified Hummers' method: 2 g of graphite was added to 50 mL of H_2SO_4 and stirred for 30 min at RT. Then, 6 g of KMnO_4 was added slowly (ice bath < 15 °C). After 2 h of stirring, 100 mL of ultra-purified distilled water (UP-DW) was added dropwise. Finally, 200 mL of UP-DW was added instantly and 10 mL of hydrogen peroxide (H_2O_2) was added dropwise to stop the reaction. Before starting characterizations, the obtained diluted acidic solution of GO was washed and centrifuged three times (10 min, 4000 rpm) and dried at 50 °C for 48 h (Figure 1). This type of sample was named GO1:3, referring to its graphite: KMnO_4 synthesis ratio. Two other samples, named GO1:2 and GO1:4, were prepared to finally obtain three types of GO samples synthesized at different mass ratios (1:2, 1:3, and 1:4; G: KMnO_4). ZnO-rGO was obtained using the reflux technique at 100 °C during 180 min. Graphene oxide and zinc acetate were dispersed and sonicated in UP-DW and DMF, respectively (GO:Zn-Ac = 1:1, DW: DMF = 1:9). After reflux reaction, our solution was washed, centrifuged, and dried in same conditions as the GO powder.

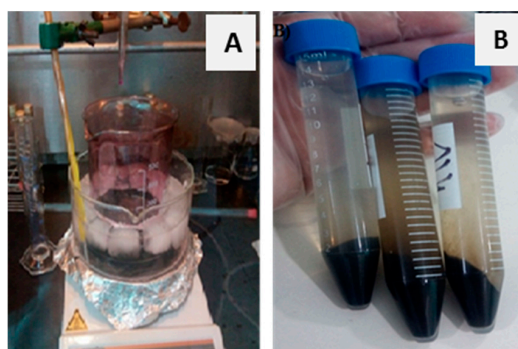


Figure 1. Image of the graphite acidic solution in ice bath during oxidation reaction (A) and the obtained pasty GO powder after centrifugation (B).

Different techniques of structural characterization were used to analyze the GO and ZnO-rGO samples. X-ray diffraction was carried out using a PanAnalytical EMPYEN diffractometer, working with $\text{CuK}\alpha$ ray ($\lambda = 1.54 \text{ \AA}$). FTIR and Raman results were obtained using FTIR-JASCO-6300 and DXR Raman spectrometers, respectively.

2.2. GO and ZnO-rGO Nanocomposites Antioxidant Activity

The antioxidant potential of tested samples was determined on the basis of their scavenging activity of the stable DPPH free radical [15]. Briefly, 0.1 mL of various concentrations of the each compound in methanol was added to 1.9 mL of a methanol solution of DPPH (0.004%). The mixture was vigorously shaken and then allowed to stand at room temperature for 30 min in the dark. The absorbance was determined at 517 nm using a Shimadzu UV-1280 spectrophotometer. Ascorbic acid was used as the positive control. All tests were performed in triplicate. The ability of scavenging DPPH radical was calculated by the following Equation (1):

$$\text{Scavenging ability (\%)} = (A_0 - A_1)/A_0 \times 100 \quad (1)$$

In the equation, A_0 is the absorbance of the control, while A_1 is the absorbance of sample.

The ability of the tested samples to scavenge H_2O_2 was estimated by the Ruch Figure method [16]. A solution of H_2O_2 (40 mM) was freshly prepared in 0.05 M KH_2PO_4 - K_2HPO_4 phosphate buffer (pH = 7.4). The compounds at different concentrations were mixed with 1.4 mL phosphate buffer and 0.6 mL 40 mM H_2O_2 . After 10 min the concentration of the H_2O_2 was determined at 230 nm using a Shimadzu UV-1280 spectrophotometer. Ascorbic acid was used as the positive control. All tests performed in triplicate. The ability of H_2O_2 neutralization was calculated using Equation (1).

3. Results and Discussion

3.1. Structural Characterizations

3.1.1. XRD

Figure 2a presents X-ray diffraction spectra of: as-received graphite powder, GO1:2, GO1:3, and GO1:4 samples. Graphite XRD spectra (recorded for comparison) display the graphite diffraction peaks with the characteristic graphite dominant peak situated at: $2\theta = 26.46^\circ$, corresponding to the diffraction of (200) planes with a d-spacing of 3.36 Å. Other low-intensity graphite diffraction peaks appear on the XRD plot, indicating the high crystallinity of the used graphite powder. XRD spectra of GO1:2, GO1:3, and GO1:4 show a disappearance of this peak mainly for GO1:4 nanocomposites. Moreover, we observe the appearance of new diffraction peaks situated at: 11.92° , 11.47° , and 11.18° , corresponding, respectively, to (001) diffraction planes of GO1:2, GO1:3, and GO1:4. As shown in Table 1, the d-spacing of the (001) XRD family plane of GO increases as function of content of KMnO_4 in the starting acidic synthesis solution.

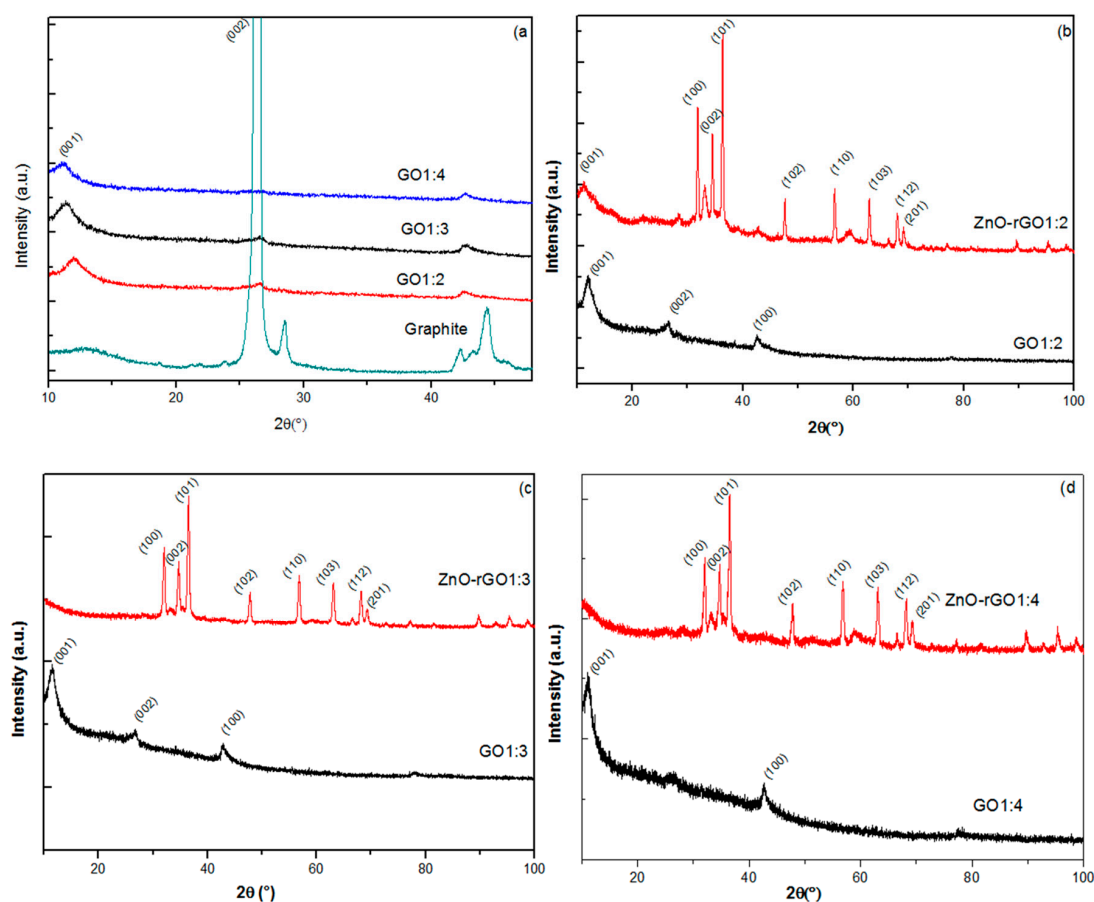


Figure 2. X-ray patterns of: (a) Graphite, GO1:2, GO1:3, and GO1:4; (b) GO1:2 and ZnO-rGO1:2; (c) GO1:3 and ZnO-rGO1:3; and (d) GO1:4 and ZnO-rGO1:4.

Table 1. D-spacing of the (100) GO diffraction plane of GO1:2, GO1:3, and GO1:4 samples.

Samples	GO1:2	GO1:3	GO1:4
2θ ($^{\circ}$)	11.92	11.47	11.18
d (\AA)	07.40	07.70	07.90

Table 1 presents the d-spacing (d_{hkl}) of the (100) GO diffraction plane of GO1:2, GO1:3 and GO1:4 samples. We indicate an increasing of d_{hkl} value with enhancement of oxidant material (potassium permanganate) in starting material of our synthesis.

Interestingly, we observe in Figure 2b–d appearance of the majority of the XRD peaks of the wurzite zinc oxide structure [JCPDS 36-1451] in all zinc oxide-decorated reduced graphene oxide samples. Simultaneously, we note the existence of the oxidation indicator peak of GO ($2\theta = 11.18^{\circ}$) in the ZnO-rGO1:2 XRD spectrum, while a total disappearance of this peak in the ZnO-rGO1:3 and ZnO-rGO1:4 spectra was observed, indicating the partial reduction of graphene oxide in ZnO-rGO1:2.

3.1.2. FTIR

FTIR results are displayed in Figure 3. For the GO1:2 plot, we observe two peaks located at 3237 cm^{-1} and 1030 cm^{-1} corresponding, respectively, to vibrations of OH and C–O bands. We note less intense peaks located at 1720 cm^{-1} and 1604 cm^{-1} indicating partial oxidation of graphite. With respect to other pristine and decorated samples, the FTIR of the GO1:3 and ZnO-rGO1:3 couple shows a large peak placed at 3230 cm^{-1} corresponding to the OH band, and in pristine GO, two sharp peaks related to C=O and C=C bands located at 1707 cm^{-1} and 1630 cm^{-1} . Interestingly, these features broaden in the GO1:4 and ZnO-rGO1:4 couple and are absent in the GO1:2 and ZnO-rGO1:2 one.

After decoration, we note a decrease in the intensity for the peak located at 3237 cm^{-1} and the total disappearance of the peak located at 1707 cm^{-1} . The FTIR spectra of the GO1:4 and ZnO-rGO1:4 samples are shown in Figure 3c. We observe the same feature found in GO1:3 and ZnO-rGO1:3, despite noting the total absence of peaks located near 3224 cm^{-1} and 1720 cm^{-1} , indicating a better reduction of GO1:4 during decoration with ZnO nanoparticles [17–19].

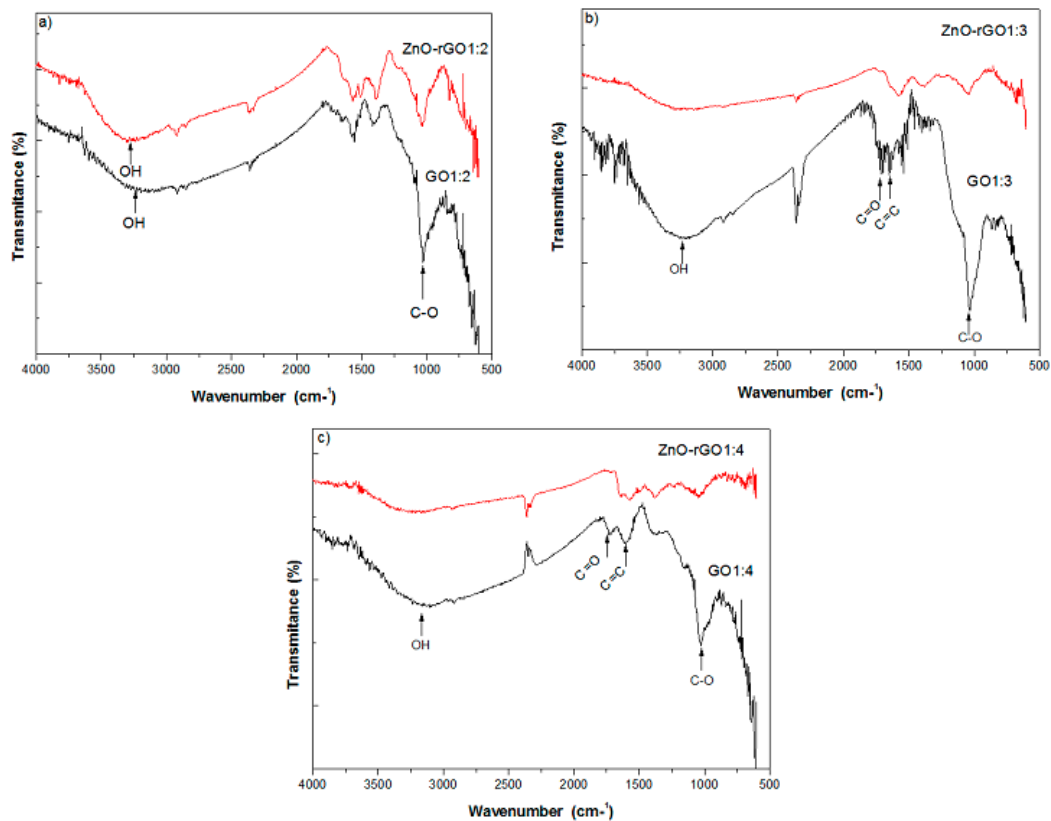


Figure 3. FTIR spectra of (a) GO1:2 and ZnO-rGO1:2; (b) GO1:3 and ZnO-rGO1:3; and (c) GO1:4 and ZnO-rGO1:4.

3.1.3. Raman

Figure 4 shows the Raman spectra of pure and zinc oxide decorated reduced graphene oxide. Raman spectra of GO1:2 and ZnO-rGO1:2 presented in Figure 4a, show D and G bands, located at 1347 cm^{-1} and 1594 cm^{-1} for both pure and decorated reduced graphene oxide in same position. These bands are attributed, respectively, to the E_{2g} vibrational mode of sp^2 carbon hybridization and structure defects [20]. We observe that the I_D/I_G ratio increases from 1.01 for GO1:2 to 1.09 for ZnO-rGO1:2 indicating a reduction of GO. We note a total absence of peaks relative to ZnO vibrational modes, probably due to our need to use a more intense laser. Similarly, we observe in Figure 4b, presenting the Raman spectra of GO1:3 and ZnO-rGO1:3 samples, D and G bands at 1340 cm^{-1} and 1589 cm^{-1} , respectively, with the respective I_D/I_G ratios of 0.96 and 1.05, indicating the reduction of GO1:3 after decoration with ZnO. We note one more time the absence of peaks relative to ZnO vibrational modes. Figure 4c provides GO1:4 and ZnO-rGO1:4 Raman spectra. D and G carbon sp^2 bands appear in the same previous positions of 1347 cm^{-1} and 1594 cm^{-1} , respectively. The I_D/I_G ratio enhances from 0.95 to 1.04 after decoration, indicating better reduction of GO1:4 after decoration with zinc oxide. Contrarily to precedent spectra of zinc oxide-decorated reduced graphene oxide, we observe a peak located at 485 cm^{-1} , corresponding to the E_2 vibrational mode of hexagonal ZnO [21], indicating a better decoration of GO with ZnO in this sample type.

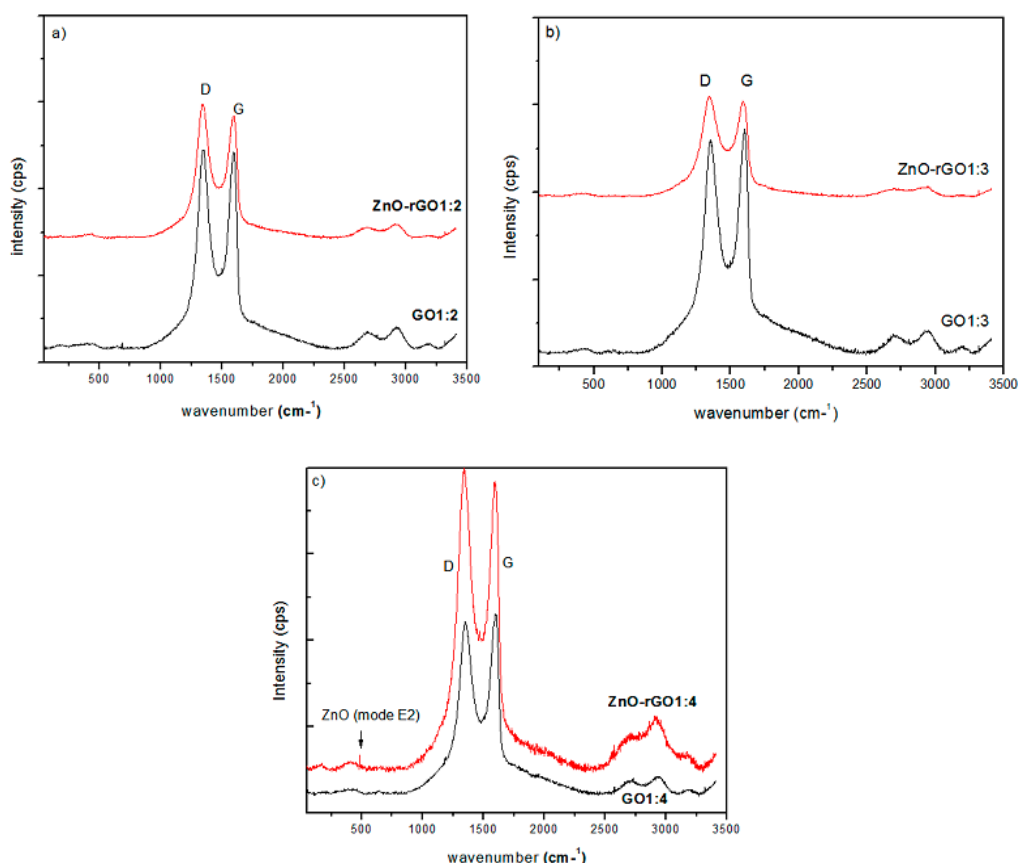


Figure 4. Raman spectra of: (a) GO1:2 and ZnO-rGO1:2; (b) GO1:3 and ZnO-rGO1:3; and (c) GO1:4 and ZnO-rGO1:4.

As a whole, the results show that the mass ratio in Hummers' method represents an important parameter for the reduction and metal oxide decoration of graphene oxide as well. In our work, we maintain more attention on the GO matrix, focusing our efforts on optimizing the GO oxidation by increasing the oxidant agent amount. As a matter of fact, the better ZnO graphene decoration corresponds to the higher oxidation degree in GO samples.

3.2. Antioxidant Assays

Recent reports have demonstrated that several types of nanoparticles act as potent free radical scavengers and antioxidants [22,23]. The prepared nanocomposites GO and ZnO-rGO were investigated for anti-oxidant properties using DPPH radical and H_2O_2 scavenging assays. In Figure 5, the ability to scavenge the DPPH radical was increased with the increase in the concentration of tested samples from 25–400 $\mu\text{g/mL}$. DPPH radical scavenging activity of different samples and ascorbic acid at 400 $\mu\text{g/mL}$ was in the following order: Ascorbic acid (96%) > GO1:4 (40%) > GO1:2 (35%) > GO1:3 (26%) > ZnO-rGO1:3 (22%) > ZnO-rGO1:2 (20%) > ZnO-rGO1:4 (19%). The DPPH assay method is based on the reduction of DPPH, a stable free radical. Antioxidants with DPPH radical scavenging activity could donate hydrogen to free radicals and to form non-radical species [15]. As observed in DPPH radical assays, the H_2O_2 scavenging ability of the tested samples was dose-dependent (Figure 6). The H_2O_2 scavenging activity of different samples and ascorbic acid at 400 $\mu\text{g/mL}$ was in the following order: Ascorbic acid (85%) > ZnO-rGO1:3 (63%) > GO 1:4 (58%) > ZnO-rGO1:2 (52%) > ZnO-rGO1:4 (47%) > GO1:2(42%) > GO1:3 (20%). H_2O_2 itself is not very reactive, but it can sometimes be toxic to the cell because it may give rise to hydroxyl radicals in the cell. Thus, removal of H_2O_2 is very essential to protecting the biological system, in general, and food components, in particular [24]. Our findings correspond with existing literature demonstrating the ability of the graphene-based family (graphene,

rGO, and GO) to neutralizing free radicals, oxygen scavenging, or peroxide decomposition through their antioxidant activities [22,25]. The antioxidant activity pattern can depend on the structure of graphene oxide or few-layer graphene [25]. Some researchers proposed that antioxidant propriety of carbon materials may involve radical adduct formation at sp² carbon sites, which delocalizes spin across the conjugated graphene backbone and leads to the destruction of the radical following second adduct formation, through electron transfer, through hydrogen donation from functional groups, or through chelation of transitional metal ions and inhibition of Fenton-based radical generation [23,24]. Interestingly, GO showed a more considerable scavenging efficiency using the DPPH radical test while the ZnO decorated GO was more efficient in the H₂O₂ antioxidant assays. The observed trend suggests the enhancement of the antioxidant activity of ZnO-rGO compared to GO, which may be due to synergetic effects or the interaction between zinc oxide nanoparticles and graphene oxide [14,25].

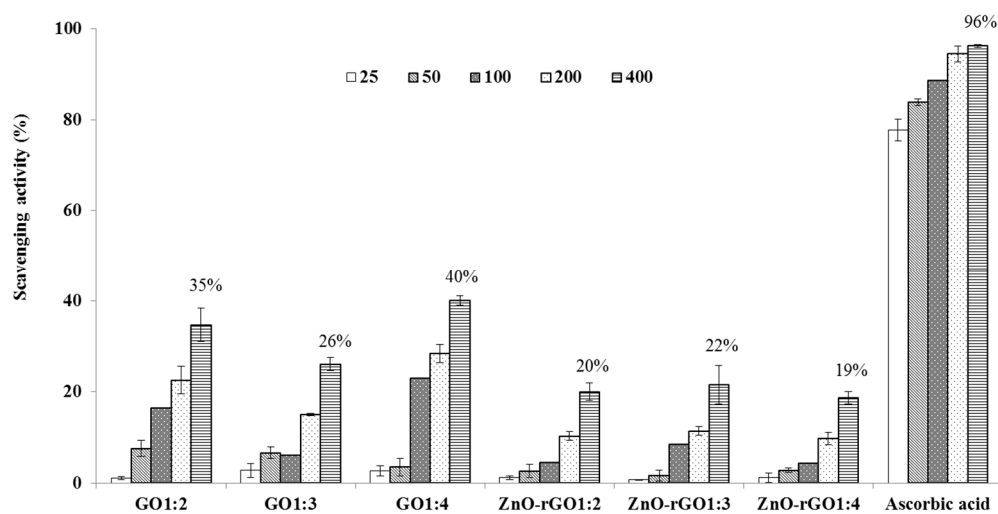


Figure 5. DPPH radical scavenging activity of GO and ZnO-rGO nanocomposites (*n* = 3). Values labeled on top of the last columns in the histogram correspond to the highest antioxidant activity reached by each sample at 400 µg.

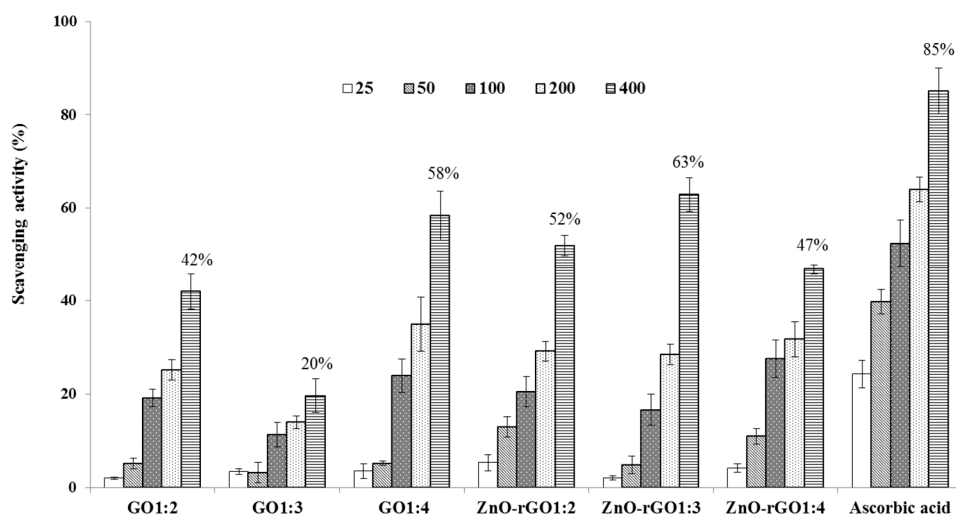


Figure 6. H₂O₂ scavenging activity of GO and ZnO-rGO nanocomposites (*n* = 3). Values labeled on top of the last columns in the histogram correspond to the highest antioxidant activity reached by each sample at 400 µg.

4. Conclusions

GO was synthesized using modified Hummers' method changing the graphite:KMnO₄ proportion. Best results in terms of the oxidation degree were obtained with a 1:4 mass ratio. XRD and Raman scattering spectra clearly indicate the reduction of GO and successful synthesis of the ZnO-rGO nanocomposite. This result has been confirmed by the appearance of peaks relative to the hexagonal wurtzite structure of ZnO. FTIR results inform us about the existence of oxygenated functional groups corresponding to hydroxyl, carboxyl, and epoxy molecules and the change of the correspondent peak intensity after the reduction of GO. Structural characterizations confirm that the better oxidized samples (GO1:4) undergo the best reduction and decoration by zinc oxide demonstrating that better-oxidized graphene oxide leads to a better reduced and decorated graphene oxide. Additionally, the prepared nanocomposites exhibited noticeable antioxidant properties. The results from DPPH radical and H₂O₂ scavenging assays revealed that GO and ZnO-rGO nanocomposites are capable of donating electrons or hydrogen atoms and, subsequently, react with free radicals in a dose-dependent manner. The ZnO-rGO nanocomposites show better H₂O₂ scavenging effects than GO. The combination of all these findings encourage simultaneously studying pure and metal oxide-decorated graphene oxide further to obtain excellent pure and metal-decorated graphene oxide matrices to check their potential biological applications. However, further exploration is necessary to determine the effective decoration degree and antioxidant capacity.

Author Contributions: Conceptualization and methodology: A.B. and G.S., and A.K.; formal analysis, investigation and resources: A.B., A.K., N.H., and N.B.; writing—original draft preparation: A.B. and N.B.; writing—review and editing: G.S.; project administration: Mentouri Brothers University and FBK-Trento.

Funding: This work was supported partially by Ministry of Higher Education and Scientific Research –Algeria (MESRS) and the Ministry of Foreign Affairs and International Cooperation of Italy; Bilateral Algerian-Italian research project AL16MO06.

Acknowledgments: We are grateful to Laid Dehimat from Mentouri Brothers University for laboratory facilities and Chawki Bensouici, Fatima Zohra Issaad, and Abdelkader Mahrouk from CRBt—Constantine for characterizations support.

Conflicts of Interest: The authors declare no conflict of interest.

References

1. Novoselov, K.S.; Geim, A.K.; Morozov, S.V.; Jiang, D.; Zhang, Y.; Dubonos, S.V.; Grigorieva, I.V.; Firsov, A.A. Electric field effect in atomically thin carbon films. *Science* **2004**, *306*, 666–669. [[CrossRef](#)] [[PubMed](#)]
2. Khan, M.M.; Cho, M.H. Green synthesis, photocatalytic and photoelectrochemical performance of an Au-graphene nanocomposite. *RSC Adv.* **2015**, *5*, 26897–26904. [[CrossRef](#)]
3. Ali, I.; Basheer, A.A.; Mbianda, X.Y.; Burakov, A.; Galunin, E.; Burakova, I.; Mkrtchyan, E.; Tkachev, A.; Grachev, V. Graphene based adsorbents for remediation of noxious pollutants from wastewater. *Environ. Int.* **2019**, *127*, 160–180. [[CrossRef](#)] [[PubMed](#)]
4. Khan, M.E.; Khan, M.M.; Cho, M.H. Recent progress of metal-graphene nanostructures in photocatalysis. *Nanoscale* **2018**, *10*, 9427–9440. [[CrossRef](#)] [[PubMed](#)]
5. Tadzyszak, K.; Wychowanec, J.K.; Litowczenko, J. Biomedical applications of graphene-based structures. *Nanomaterials* **2018**, *8*, 944. [[CrossRef](#)]
6. Alam, S.N.; Sharma, N.; Kumar, L. Synthesis of graphene oxide by modified Hummers method and its thermal reduction to obtain reduced graphene oxide. *Graphene* **2017**, *6*, 1–18. [[CrossRef](#)]
7. Marcano, D.C.; Kosynkin, D.V.; Berlin, J.M.; Sinitskii, A.; Sun, Z.; Slesarev, A.; Alemany, L.B.; Lu, W.; Tour, J.M. Improved synthesis of graphene oxide. *ACS Nano.* **2010**, *4*, 4806–4814. [[CrossRef](#)]
8. Omar, F.S.; Ming, H.N.; Hafiz, S.M.; Ngee, L.H. Microwave synthesis of zinc oxide/reduced graphene oxide hybrid for adsorption-photocatalysis application. *Int J. Photoenergy* **2014**, *2014*, 176835. [[CrossRef](#)]
9. Parnianchi, F.; Nazari, M.; Maleki, J.; Mohebi, M. Combination of graphene and graphene oxide with metal and metal oxide nanoparticles in fabrication of electrochemical enzymatic biosensors. *Int. Nano Lett.* **2018**, *8*, 229–239. [[CrossRef](#)]

10. Papageorgiou, D.G.; Kinloch, I.A.; Young, R.J. Mechanical properties of graphene and graphene-based nanocomposites. *Prog. Mater. Sci.* **2017**, *90*, 75–127. [[CrossRef](#)]
11. Khan, M.E.; Khan, M.M.; Cho, M.H. Biogenic, synthesis of Ag–graphene nanocomposite with efficient photocatalytic degradation, electrical conductivity and photoelectrochemical performance. *New J. Chem.* **2015**, *39*, 8121–8129. [[CrossRef](#)]
12. Siddeswara, D.M.K.; Vishnu Mahesh, K.R.; Sharma, S.C.; Mylarappa, M.; Nagabhushana, H.; Ananthraju, K.S.; Nagaswarupa, H.P.; Prashantha, S.C.; Raghavendra, N. ZnO decorated graphene nanosheets: An advanced material for the electrochemical performance and photocatalytic degradation of organic dyes. *Nanosyst. Phys. Chem. Math.* **2016**, *7*, 678–682. [[CrossRef](#)]
13. Durmus, Z.; Kurt, B.Z.; Durmus, A. Synthesis and characterization of graphene oxide/zinc oxide (GO/ZnO) nanocomposite and its utilization for photocatalytic degradation of basic Fuchsin dye. *ChemistrySelect* **2019**, *4*, 271–278. [[CrossRef](#)]
14. Shadmehri, A.A.; Namvar, F.; Miri, H.; Yaghmaei, P.; Moghaddam, M.N. Assessment of antioxidant and antibacterial activities of zinc oxide nanoparticles, graphene and graphene decorated by zinc oxide nanoparticles. *Int. J. Nano Dimens.* **2019**, *10*, 395–403.
15. Blois, M.S. Antioxidant determinations by the use of a stable free radical. *Nature* **1958**, *181*, 1199–1200. [[CrossRef](#)]
16. Ruch, R.J.; Cheng, S.J.; Klaunig, E. Prevention of cytotoxicity and inhibition of intercellular communication by antioxidant catechins isolated from Chinese green tea. *Carcinogenesis* **1989**, *10*, 1003–1008. [[CrossRef](#)]
17. Farhanini, Y.; Khing, N.T.; Hao, C.C.; Sang, L.P.; Basyirah, M.N.; Noorashikin, M.S. The electrochemical behavior of zinc oxide/reduced graphene oxide composite electrode in dopamine. *Malays. J. Anal. Sci.* **2018**, *22*, 227–237.
18. Moon, I.K.; Lee, J.; Ruoff, R.S.; Lee, H. Reduced graphene oxide by chemical graphitization. *Nat. Commun.* **2010**, *1*, 73. [[CrossRef](#)]
19. Kim, K.S.; Rhee, K.Y.; Park, S.J. Influence of multi-walled carbon nanotubes on the electrochemical performance of transparent graphene electrodes. *Mater. Res. Bull.* **2011**, *46*, 1301–1306. [[CrossRef](#)]
20. Zhong, X.; Jin, J.; Li, S.; Niu, Z.; Hu, W.; Li, R.; Ma, J. Aryne cycloaddition: Highly efficient chemical modification of graphene. *Chem. Commun.* **2010**, *46*, 7340–7734. [[CrossRef](#)]
21. Lo, S.S.; Huang, D.; Tu, C.H.; Jan, D.J. Formation and Raman scattering of seed-like ZnO nanostructure. *J. Raman Spectrosc.* **2009**, *40*, 1694–1697. [[CrossRef](#)]
22. Qiu, Y.; Wang, Z.; Owens, A.C.; Kulaots, I.; Chen, Y.; Kane, A.B.; Hurt, R.H. Antioxidant chemistry of graphene-based materials and its role in oxidation protection technology. *Nanoscale* **2014**, *6*, 11744–11755. [[CrossRef](#)] [[PubMed](#)]
23. Lee, Y.M.; Yoon, Y.; Yoon, H.; Song, S.; Park, H.M.; Lee, Y.Y.; Shin, H.; Hwang, S.W.; Yeum, K.J. Enhanced antioxidant activity of bioactives in colored grains by nano-carriers in human lens epithelial cells. *Molecules* **2018**, *23*, 1327. [[CrossRef](#)] [[PubMed](#)]
24. Rajeswari, R.; Prabu, H.G. Synthesis characterization, antimicrobial, antioxidant, and cytotoxic activities of ZnO nanorods on reduced graphene oxide. *J. Inorg. Organomet. Polym.* **2018**, *28*, 679–693. [[CrossRef](#)]
25. Suresha, D.; Pavan Kumarb, M.A.; Nagabhushan, H.; Sharma, S.H. Cinnamon supported facile green reduction of graphene oxide, its elimination and antioxidant activities. *Mater. Lett.* **2015**, *151*, 93–95. [[CrossRef](#)]

